




# Influence of hydrothermal pretreatment and hydrochar addition on enhanced anaerobic digestion of various biomass

Apatsorn Khongyarit<sup>a</sup>, Navadol Laosiripojana<sup>b</sup>, Santhana Krishnan<sup>a,c</sup>, Sucheewan Yoyrurob<sup>d</sup>, Boonya Charnnok<sup>a,\*</sup> 

<sup>a</sup> Energy Technology Program, Department of Interdisciplinary Engineering, Faculty of Engineering, Prince of Songkla University, Hat Yai, Songkhla, 90110, Thailand

<sup>b</sup> The Joint Graduate School for Energy and Environment (JGSEE), King Mongkut's University of Technology Thonburi, Prachautit Road, Bangmod, Bangkok, 10140, Thailand

<sup>c</sup> Environmental Technology Division, School of Industrial Technology, Universiti Sains Malaysia, Penang, 11800, Malaysia

<sup>d</sup> Faculty of Science and Technology, Songkhla Rajabhat University, Mueang Songkhla District, Songkhla, 90000, Thailand

## ARTICLE INFO

### Keywords:

Anaerobic digestion  
Hydrochar addition  
Hydrothermal pretreatment  
Lignocellulosic biomass  
Starchy biomass  
Waste oil

## ABSTRACT

This study evaluated the effects of hydrothermal pretreatment (50–150 °C) and hydrochar addition (2.5–10 %) on the anaerobic digestion of grass silage (GS), starchy residues (SR, LCR), and waste oil (WO). Hydrothermal pretreatment at 150 °C significantly increased methane yield from GS, but reduced performance for starchy residues, indicating that its effectiveness is highly substrate-dependent. In contrast, hydrochar derived from digestate (HD), owing to its higher surface area, ash content, and electrical conductivity, outperformed hydrochar from *Leucaena* residue. The combined application of 10 % HD and hydrothermal pretreatment accelerated early-stage methanogenesis but lowered cumulative methane yields after 35 days. Importantly, hydrochar addition alone improved or maintained methane yield across all substrates, and for GS it provided an alternative to hydrothermal pretreatment. Optimal hydrochar dosages—5 % for Un-GS and Un-LCR, 2.5 % for Un-SR, and 5 % for WO—enhanced methane yields (e.g., +19.2 % for GS, +7.4 % for LCR) and maintained yields for Un-SR and WO. These findings highlight the need for substrate-specific pretreatment strategies and support the transition of conventional biogas plants toward net-zero emissions by integrating energy generation with nature-based carbon sequestration.

## 1. Introduction

Thailand aims to achieve net-zero emissions by 2065, emphasizing renewable energy expansion. As of 2022, renewables comprised 13.38 % of the energy mix, targeting 30 % by 2037. Anaerobic digestion (AD) supports this goal by converting biomass into biogas, with energy security relying on steady feedstock supply and process efficiency. Currently, Thailand's biogas power plants utilize two primary feedstock types: wastewater and lignocellulosic biomass, with *Napier* grass being the most widely used. However, *Napier* grass cultivation faces limitations due to inefficient biogas yields and feedstock shortages, land competition with food crops.

*Napier* grass contains high cellulose (37.1–44.1 %) and hemicellulose (24.6–25.7 %), but its lignin content (19.4–23.8 %) [1,2] limits microbial hydrolysis, slowing acidogenesis and acetogenesis, and ultimately

constraining methanogenesis. Hydrothermal pretreatment offers a promising approach to enhance AD efficiency by breaking down complex biomass structures particularly hemicellulose and cellulose into more readily degradable compounds such as xylose, arabinose, glucose [3]. Low-temperature hydrothermal pretreatment (50–150 °C) can improve digestibility through break down hemicellulose [4] while utilizing waste heat from industrial processes or solar thermal energy, thereby reducing pretreatment costs and greenhouse gas emissions. Numerous studies have reported the benefits of hydrothermal pretreatment on various organic wastes such as food waste [5], sludge [6], slaughterhouse waste [7], animal manure [8], lignocellulosic biomass [9], pulp waste [10].

In parallel, carbonaceous additives such as biochar and hydrochar have been explored for enhancing AD via direct interspecies electron transfer (DIET), improving electron exchange between fermentative

\* Corresponding author. Energy Technology Program, Department of Interdisciplinary Engineering, Faculty of Engineering, Prince of Songkla University, Hat Yai, Songkhla, 90110, Thailand.

E-mail address: [boonya.c@psu.ac.th](mailto:boonya.c@psu.ac.th) (B. Charnnok).

<https://doi.org/10.1016/j.biombioe.2025.108431>

Received 28 June 2025; Received in revised form 4 September 2025; Accepted 23 September 2025

Available online 1 October 2025

0961-9534/© 2025 Elsevier Ltd. All rights are reserved, including those for text and data mining, AI training, and similar technologies.

bacteria and methanogenic archaea, particularly along hydrogenotrophic pathways [11,12]. The large surface area of these materials further supports microbial attachment and biofilm formation, promoting microbial activity and diversity [12]. Furthermore, digestate from Napier grass-fed biogas plants is often applied as a soil amendment, but its volatile solids content can continue degrading anaerobically after land application, releasing methane and undermining net-zero goals. Hydrochar, a stable carbon-rich material produced via hydrothermal carbonization under subcritical water (HTC, 100–347 °C), offers additional benefits. Converting digestate into hydrochar not only promotes methane production when reapplied in AD systems as part of a circular bioeconomy, but also stabilizes carbon for long-term sequestration and reduces phytotoxicity when subsequently utilized as a soil amendment [13]. However, previous studies report conflicting effects of carbon additives on methane production depending on biomass type, hydrochar characteristics and hydrochar dosage [14–16], posing challenges for full-scale biogas operations if hydrochar addition method is applied.

Additionally, Thailand generates substantial amounts of starchy waste (e.g., spoiled rice (SR) and leftover cooked rice (LCR)) and waste oil (WO), which are often discarded due to insufficient reuse options. Utilizing these wastes as co-substrates offers a promising solution to supplement Napier grass shortages in biogas plants, while reducing operational and investment costs compared to constructing separate facilities for food waste or WO digestion. However, before implementing such co-digestion strategies, it is critical to understand the distinct degradation characteristics of each biomass type to ensure process stability and optimize overall methane production efficiency.

Therefore, this study investigated the effects of low-temperature hydrothermal pretreatment (50–150 °C) and hydrochar addition on the anaerobic digestion of grass silage (GS), starchy biomass (SR and LCR), and WO. Two hydrochars—derived from digestate and *Leucaena* residues—were evaluated for their potential to enhance methane production. The findings aim to support the design of co-digestion strategies to mitigate Napier grass shortages and improve management of starchy waste and WO, while simultaneously advancing renewable energy generation and nature-based carbon sequestration.

## 2. Materials and methods

### 2.1. Hydrothermal carbonization

Real digestate was collected from a full-scale biogas power plant. *Leucaena* residues were obtained from *Leucaena* plants, which were agricultural by-products. *Leucaena* residues were left in the field after the biomass had been harvested for sale to a biomass power plant, while the leaves were used as animal feed. These *Leucaena* plants were in Khun Tad Wai sub-district, Chana district, Songkhla province. *Leucaena* residues were chopped to a size of 1 cm. Both feedstocks were dried at 60 °C before being individually subjected to hydrochar production via HTC.

The HTC process was conducted in a laboratory-scale pressurized reactor (P.T. Scientific Co., Ltd., Thailand) with a capacity of 500 mL. The reactor was equipped with a temperature probe and a pressure gauge connected to a pressure transmitter for monitoring internal conditions. The reaction was performed at 265 °C for 60 min, with a working volume of 250 mL (containing 25 g of biomass) and a feedstock-to-distilled water ratio of 1:10 w/v. During the process, the reactor pressure for the HTC of *Leucaena* residues and digestate reached  $50.37 \pm 0.80$  bar and  $49.93 \pm 0.25$  bar, respectively. Mixing was maintained at 100 rpm. After the reaction, the liquid phase was separated from the hydrochar. The yields of the *Leucaena* derived hydrochar (HL) and digestate derived hydrochar (HD) were calculated using Eq. (1), and their characteristics were subsequently analyzed (Table 1).

$$\text{Hydrochar yield (\%)} = \frac{\text{Hydrochar (g)}}{\text{Feedstock (g)}} \times 100 \quad (1)$$

**Table 1**  
Characteristics of hydrochar.

Parameter	<i>Leucaena</i> derived hydrochar <sup>a</sup>	Digestate derived hydrochar <sup>b</sup>
Hydrochar yield	48.4 ± 0.50	45.6 ± 1.7
<b>Proximate analysis (% wt.)</b>		
Moisture content	1.30 ± 0.02	–
Volatile solid	53.02 ± 0.10	40.1 ± 0.2
Fixed carbon	41.36 ± 0.15	23.1 ± 0.1
Ash	4.31 ± 0.15	36.8 ± 0.2
<b>Ultimate analysis (% wt.)</b>		
Carbon	66.19 ± 0.56	40.6 ± 0.4
Hydrogen	5.55 ± 0.06	3.5 ± 0.1
Oxygen	22.57 ± 0.12	15.9 ± 0.6
Nitrogen	1.99 ± 0.03	2.8 ± 0.0
Sulfur	0.11 ± 0.00	0.4 ± 0.0
H/C	1.00	1.03
O/C	0.26	0.29
Thermostable fraction (%)	43.82	36.56
Surface area (m <sup>2</sup> /g)	5.75	27.23
Total pore volume (cm <sup>3</sup> /g)	0.019	0.11
Average pore diameter (nm)	12.95	16.82
Electrical conductivity (mS/cm)	5.11 ± 0.04	8.21 ± 0.01
<b>Elements (% wt.)</b>		
Mg	0.456	2.76
Al	0.096	0.555
Si	0.312	10.61
P	1.18	6.53
S	0.399	1.24
Cl	0.733	0.475
K	2.07	ND
Ca	1.57	12.58
Fe	0.078	0.659
Cu	0.010	0.009
Zn	0.009	0.029
Na	0.053	ND
Ti	ND	0.052
Mn	0.029	0.099
Rb	0.003	0.007
Cr	ND	0.019
Ni	0.006	0.011
Sr	0.003	0.012

Note: ND = not detected.

<sup>a</sup> Data for *Leucaena*-derived hydrochar sourced from Charnnok et al. [17] and Pengpit et al. [18], except for electrical conductivity and elemental composition, which were additionally analyzed in this study.

<sup>b</sup> Data for digestate-derived hydrochar sourced from Charnnok et al. [17] except for elemental composition, which was additionally analyzed in this study.

### 2.2. Feedstock preparation for anaerobic digestion

The energy crop and bio-waste used for anaerobic digestion are described, and their characteristics are presented in Table 2.

- Napier grass silage (GS): A mixture of GS A mixture of Napier grass silage (aged 90 days) and corn residue silage (aged 60 days) was prepared in an 80:20 w/w ratio. The GS was then milled to reduce its size to 0.2 mm and subsequently dried at 60 °C until a constant weight was achieved.
- Starchy food waste: Jasmine rice (*Oryza sativa* L.) served as the base for the starchy food waste. SR was used as it had deteriorated after prolonged storage. It was ground into a fine powder. LCR was used, which refers to the rice that was cooked but not consumed and subsequently discarded. The rice was cooked for 1 h, then dried and ground into a fine powder. Both SR and LCR were dried at 60 °C until they reached a constant weight.

**Table 2**  
Characteristics of feedstock.

Parameter	GS	SR	LCR	WO
Proximate analysis (%)				
Moisture (in wet)	72.63 ± 2.01	8.84 ± 0.13	67.46 ± 0.48	43.04 ± 9.28
TS (in wet)	27.37 ± 2.01	91.16 ± 0.13	32.54 ± 0.48	56.96 ± 9.28
VS (in TS)	93.14 ± 0.81	98.01 ± 0.53	98.23 ± 0.28	94.80 ± 0.77
Ash (in TS)	6.86 ± 0.81	1.99 ± 0.53	1.77 ± 0.28	5.20 ± 0.77
Ultimate analysis (%)				
Carbon	45.12 ± 0.04	38.68 ± 0.03	37.94 ± 0.04	N/A
Hydrogen	5.83 ± 0.07	6.33 ± 0.12	5.99 ± 0.06	N/A
Oxygen	41.96 ± 0.22	51.82 ± 0.23	49.73 ± 0.22	N/A
Nitrogen	0.68 ± 0.02	1.11 ± 0.02	1.07 ± 0.02	N/A
Sulfur	0.06 ± 0.00	0.06 ± 0.00	0.05 ± 0.00	N/A
Carbon/Nitrogen	66.35	34.85	35.46	N/A
Theoretical methane (LCH <sub>4</sub> /kg VS)	461.10	355.70	358.40	640.00
Higher heating value (MJ/kg)	16.45 ± 23.6	13.41 ± 1.21	13.53 ± 0.77	N/A
Lower heating value (MJ/kg)	15.19 ± 20.2	12.02 ± 1.14	12.15 ± 0.74	N/A
Element content (%)				
Mg	0.526	0.021	0.016	N/A
Al	0.144	0.004	0.004	N/A
Si	4.529	0.008	0.013	N/A
P	0.443	0.081	0.079	N/A
S	0.266	0.078	0.085	N/A
Cl	0.897	0.046	0.056	N/A
K	3.131	0.084	0.102	N/A
Ca	0.846	0.005	0.005	N/A
Fe	0.156	0.004	0.005	N/A
Cu	0.011	0.006	0.006	N/A
Zn	0.010	0.002	0.003	N/A
Na	0.012	ND	ND	N/A
Ti	0.017	ND	ND	N/A
Mn	0.056	ND	ND	N/A
Br	0.062	ND	ND	N/A
Rb	0.025	ND	ND	N/A
Cr	0.010	ND	ND	N/A
Ni	ND	ND	ND	N/A
Pb	ND	ND	ND	N/A
Sr	0.003	ND	ND	N/A

Note: Grass silage, GS; Spoiled rice, SR; Left-over cooked rice, LCR; Waste oil, WO; ND, not detected; N/A, not applicable; Values are presented as means ± standard deviations.; Theoretical methane yield of WO was estimated using Eq. (5), assuming it was fat and normalized to VS.

- WO: WO used is oil that was separated from wastewater treatment pond in a seafood processing factory. It was stored at 4 °C for a short period prior to the start of the study. It did not undergo any pre-treatment before being used in the experiment.

### 2.3. Hydrothermal pretreatment

The hydrothermal pretreatment of GS, SR, and LCR was performed in triplicate at three different temperatures: 50 °C, 100 °C, and 150 °C. Each biomass was mixed with distilled water at a ratio of 16.1 % w/v. The reaction times were selected to ensure a comparable reaction progress across different temperatures. For the 50 °C treatment, the mixtures of 85 mL were placed in 250 mL glass reactors. The reactors were incubated in a shaking incubator (Model NB-205) at 100 rpm for 20 h. This is consistent with previous studies showing that lower

temperatures require longer reaction times to achieve desired results [4]. For the 100 °C and 150 °C treatments (for 3 h retention time), the process was conducted in a laboratory-scale pressurized reactor with a volume of 500 mL (biomass 40.85 g and distilled water 250 mL). Mixing was maintained at 100 rpm throughout the reaction.

After pretreatment, the samples were allowed to cool to room temperature (30 °C). The pH, total solids (TS), and volatile solids (VS) of the mixtures were then analyzed. The mixtures were also subjected to biochemical methane potential (BMP) assay. Additionally, the liquid was filtered through a nylon syringe filter (0.22 µm) and analyzed using high-performance liquid chromatography (HPLC) to determine the content of sugars, organic acids, furfural, and 5-hydroxymethylfurfural (5-HMF).

### 2.4. Biochemical methane potential assay

The effects of hydrothermal pretreatment (50 °C (12 h), and 100 °C (3 h) and 150 °C (3 h)) and hydrochar addition (2.5, 5 and 10 % of substrate dry mass) on the methane potential of GS, SR, LCR, and WO were investigated using a batch BMP assay. The study procedure is illustrated in Figure S-1.

Anaerobic digestion was carried out in triplicate, using sealed batch reaction vessels with a total volume of 26 mL. The effective reaction volume was 14 mL, leaving a headspace of 12 mL. The vessels contained 0.2 g TS substrate, and the inoculum-to-substrate ratio was 2:1 on a TS basis. The inoculum used was sludge collected from a full-scale anaerobic digester treating wastewater from a palm oil mill factory in Satun Province, Thailand. To the inoculum-substrate mixtures, 10 % (v/v) of buffer solution (50 g/L NaHCO<sub>3</sub>) and 1 % (v/v) of a macro- and microelement solution were added, following [19]. The pH of the mixture was adjusted to between 6.8 and 7.2 using hydrochloric acid (1 M). Distilled water was then added to achieve a final volume of 14 mL. To create anaerobic conditions, the air inside the bottles was purged with nitrogen gas. The samples were incubated at 35 °C with shaking at 135 rpm. The incubation period was 35 days for GS, SR, and LCR. For WO, a 35-day incubation was used for comparative analyses, ensuring a consistent duration for all substrates. Additionally, a longer 58-day incubation was performed to evaluate WO's final methane potential without hydrochar addition, as methane production from WO continued beyond the 35-day period.

Gas pressure was measured daily using a Lutron manometer (Model PM-9110SD). The biogas volume was calculated using Eq. (2), and the methane concentration in the biogas was analyzed using a Hewlett-Packard 6890 gas chromatograph equipped with a thermal conductivity detector and an HP-PLOT Q column (0.53 mm ID × 30 m length, 40 µm film), using helium as the carrier gas. Methane production was calculated using Eq. (3) and reported as normalized to standard temperature and pressure (STP).

$$V_1 = \frac{P_2 V_2 T_1}{T_2 P_1} \quad (2)$$

$P_1$  = atmospheric pressure at 1 atm, which is equal to 1013.25 mbar,  $V_1$  = volume of biogas (mL),  $T_1$  = temperature at 0 °C (273.15 K),  $P_2$  = measured gas pressure (mbar),  $V_2$  = remaining volume in the bottle (mL),  $T_2$  = temperature at 35 °C (308.15 K)

$$\text{Methane yield} \left( \frac{\text{L CH}_4}{\text{kg VS}} \right) = \frac{\text{volume of biogas (L)} \times \text{CH}_4 \text{ content (\%)}}{\text{mass of volatile solid (kg)}} \quad (3)$$

Theoretical methane yields for each feedstock were calculated. For GS, SR, and LCR, the theoretical yields at STP were determined using Eq. (4) [20]. For WO, because its elemental content could not be fully analyzed, the theoretical methane yield (640 L CH<sub>4</sub>/kg VS) was calculated from Eq. (5) [21], assuming it to be fat and normalized to VS (excluding moisture and ash). This value represents the theoretical upper bound, since WO also contains non-lipid organic matter. Biodegradability was then calculated as the ratio of the experimentally

measured methane yield from BMP assays to its corresponding theoretical methane yield (Eq. (6)) [22]. Additionally, percentage improvements of methane yield were calculated based on the experimentally measured yields from the BMP assays.

$$C_c H_h O_o N_n S_s \rightarrow \frac{1}{4}(4c - h - 2o + 3n + 2s)H_2O + \frac{1}{8}(4c - h + 2o + 3n + 2s)CO_2 + \frac{1}{8}(4c - h + 2o + 3n + 2s)CH_4 + nNH_3 + sH_2S \quad (4)$$

where c, h, o, n, s are the result of the elemental analysis.

$$\text{Theoretical methane of fat} = C_{12}H_{24}O_6 + 3H_2O \rightarrow 4.5CO_2 + 7.5CH_4 \quad (5)$$

$$\text{Biodegradability (\%)} = \frac{\text{Experimental } CH_4 \text{ yield}}{\text{Theoretical methane yield}} \times 100 \quad (6)$$

The modified Gompertz model (Eq. (7)) were applied to estimate the methane production kinetics of the biomass. The model parameters were determined by minimizing the least-square differences between the observed and predicted values.

$$B = P \times \exp \left[ - \exp \left[ \frac{R_m \times e}{B_0} (\lambda - t) + 1 \right] \right] \quad (7)$$

where  $P$  denotes the cumulative methane production (L  $CH_4$ /kg-VS);  $t$  is the time of the assay (day);  $k_0$  is the specific rate constant ( $\text{day}^{-1}$ );  $e$  is Euler's number, i.e., 2.7183;  $\lambda$  denotes the lag phase (days); and  $R_m$  is the methane production rate (L  $CH_4$ /day).

## 2.5. Analytical method

The feedstock and hydrochar were subjected to the analysis of CHONS using a CHNS/O Analyzer, FLASH 2000, ThermoScientific, Italy. Surface morphology was characterized using a scanning electron microscope (SEM-Quanta). BET surface area, total pore volume and average pore diameter were analyzed using a specific surface area analyzer, Belsorp, mini II. The functional groups were identified using a Fourier Transform Infrared Spectroscopy (FTIR) with the KBr pellet technique, using a Vertex 70 (Bruker, Germany). The elemental content was analyzed using an X-ray Fluorescence Spectrometer (Zetium, PANalytical, Netherlands) and a Simultaneous Thermal Analyzer (STA8000, PerkinElmer, USA).

The concentration of organic acids, furfural, hydroxymethylfurfural, and sugars in the pretreated sample and digestate were analyzed using HPLC (Agilent 1100; Agilent Technologies Co., Ltd.) with a diode array detector and refractive index detector. The HPLC was equipped with an Aminex HPX-87H (7.8-mm column and 300 mm in length; Bio-Rad Laboratories Ltd.). In addition, 0.005 M  $H_2SO_4$  was used as the mobile phase and at a flow rate of 0.6 mL/min [23]. Lastly, total organic carbon was determined using a TOC analyzer (multi N/C 3100, Analytik Jena AG, Germany).

## 2.6. Statistical analysis

Statistical analysis was performed using analysis of variance. Post hoc comparisons were conducted using Fisher's least significant difference method. Statistical significance was determined at  $p < 0.05$ . All data analyses were carried out using Microsoft® Excel for Mac, version 16.58 (22021501).

## 3. Results and discussion

### 3.1. Effects of hydrothermal pretreatment on anaerobic digestion

The effects of hydrothermal pretreatment on methane yield were evaluated for GS, SR, and LCR and compared to untreated WO.

Pretreatment significantly improved methane production from GS, which contains a more recalcitrant lignocellulosic structure than starchy biomass. Increasing the pretreatment temperature from 50 °C to 100 °C and 150 °C enhanced methane yield by 11.4 % and 30.5 %, respectively (Fig. 1). This improvement was attributed to the thermal breakdown of  $\beta$ -glycosidic linkages, hydrogen bonds, and covalent bonds in hemicellulose, cellulose, and lignin, leading to the release of sugars and organic acids that are more readily utilized in acidogenesis and acetogenesis—stages that operate more efficiently at elevated temperatures. Hemicellulose, being particularly heat-sensitive [24], contributed to a 2.53-fold increase in xylose and a 1.35-fold increase in glucose between 50 °C and 150 °C. Xylose and arabinose were the dominant sugars detected, followed by glucose (Table 3). Additionally, acetic acid—a key intermediate for methanogenesis—was most abundant at 150 °C, promoting methane formation via the acetoclastic pathway. The remaining solids served as secondary carbon sources, requiring further hydrolysis during digestion [25]. As a result, GS-150 achieved the highest methane yield ( $184.71 \pm 4.24$  L  $CH_4$ /kg VS).

In contrast to GS, hydrothermal pretreatment reduced methane yields from SR and LCR. As starch-based biomasses, SR and LCR were more thermally labile, leading to higher concentrations of furfural and 5-HMF compared to GS—compounds known to inhibit microbial activity [26]. Additionally, hexanoic acid, a product of chain elongation involving ethanol or lactate and acetate, was detected in the digestate of LCR (Table S-1). This likely resulted from the rapid glucose release during pretreatment. Although its concentration did not lower pH to inhibitory levels (6.93–7.32), the formation of hexanoic acid may have competed with methanogens for acetate, reducing its availability for the acetoclastic pathway. This shift toward the hydrogenotrophic pathway, which generally proceeds more slowly, may have further limited methane production [27]. Therefore, the use of untreated SR and LCR is recommended to maintain higher methane yields.

Interestingly, Un-SR ( $292.24 \pm 1.99$  L  $CH_4$ /kg VS) produced 8.7 % more methane than Un-LCR ( $268.96 \pm 0.51$  L  $CH_4$ /kg VS), likely due to higher total organic carbon (TOC) release. TOC analysis showed  $1.22 \pm 0.06$  g TOC/L in Un-SR leachate, compared to  $0.80 \pm 0.02$  g TOC/L in Un-LCR (the biomass powder with DI water at a ratio of 1:6.12 (w/v), and shaking for 30 min before analyzing the total organic carbon in the liquid fraction.). The intact starch granules in Un-SR allowed easier carbohydrate leaching, while gelatinization in Un-LCR resulted in a compact structure that restricted TOC solubilization.

When comparing the highest-yielding experimental samples of each biomass type (GS-150, Un-SR, and Un-LCR) after 35 days of digestion, their methane yields were 58.7 %, 34.7 %, and 39.9 % lower than that of WO ( $447.49 \pm 24.27$  L  $CH_4$ /kg VS), respectively. These comparisons were made at 35 days because methane production from GS, SR, and LCR had already plateaued, whereas WO continued producing methane beyond this period. The final experimental methane yield of WO reached  $507.61 \pm 9.37$  L  $CH_4$ /kg VS at 58 days, equivalent to 13.43 % of the yield obtained within 35 days, indicating the extended methane potential of WO. WO's superior performance is attributed to its higher carbon content; however, its high lipid content prolonged the lag phase ( $\lambda$ ) (Table 4), reflecting the slow hydrolysis of lipids and the associated requirement for larger digester capacity.

### 3.2. Comparison of hydrochar additive in anaerobic digestion of pretreated biomass

The combined effects of hydrothermal pretreatment and hydrochar addition (10 % of feedstock on a dry basis) on methane yield were evaluated using two types of hydrochar: HL and HD. GS-150 provided the highest methane yield among all pretreatment conditions, while 150 °C was also selected for SR and LCR to enable consistent comparison. These three pretreated biomasses were further compared with WO to evaluate the effects of hydrochar addition across diverse substrate types.



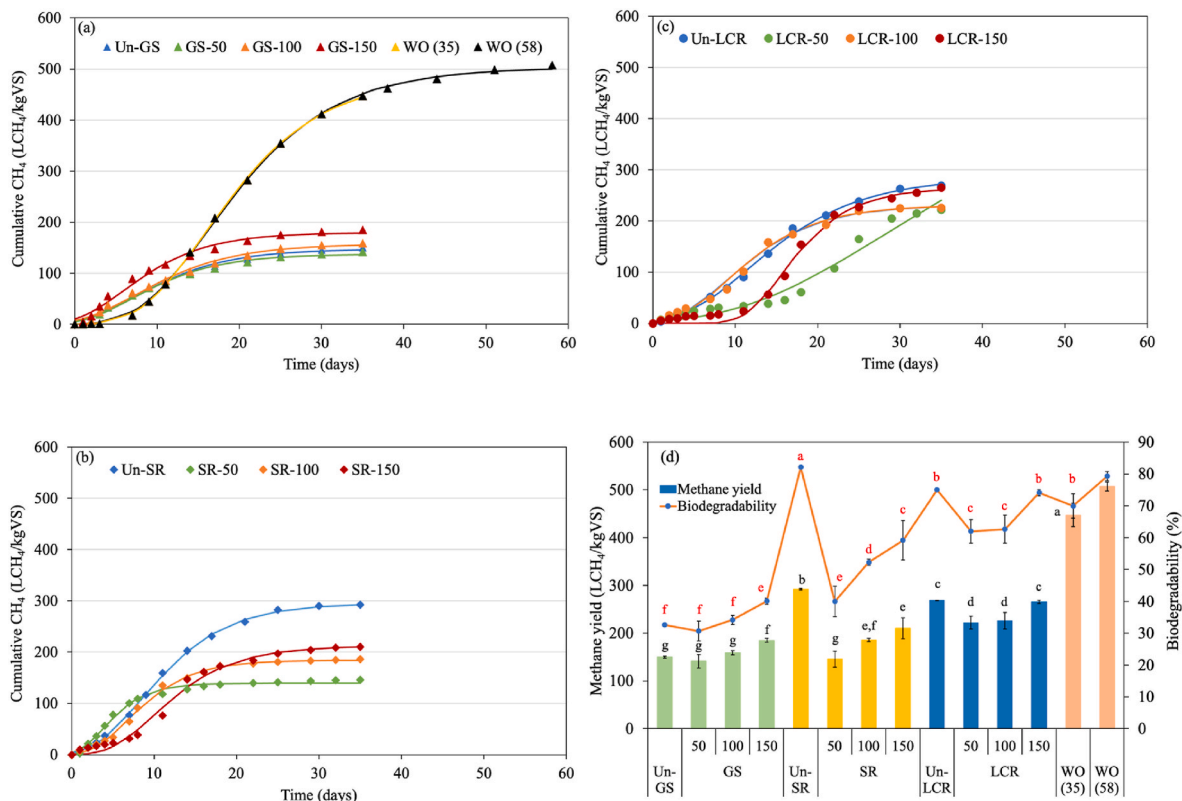


**Fig. 1.** Anaerobic digestion of untreated biomass and pretreated biomass (a) GS and WO, (b) SR, (c) LCR, (d) methane yield and biodegradation.

Note: Grass silage, GS; Spoiled rice, SR; Left-over cooked rice, LCR; Waste oil, WO; The methane yields shown for all biomass types are from a 35-day incubation period, with the exception of the WO (58) sample, which shows the final yield after a 58-day incubation. The WO (58) data were not subjected to statistical analysis due to the different incubation periods.; Different letters indicate significant differences with  $p \leq 0.05$  for methane yield.

Both types of hydrochar positively influenced the methanogenesis phase of all types of feedstocks, as evidenced by a shorter  $\lambda$  compared to the sample without hydrochar (Table 5). Notably, methane content and cumulative methane yield in hydrochar-amended samples exceeded those of the sample without hydrochar at earlier incubation times—5 days for GS-150, and 10 days for SR-150, LCR-150, and WO (Fig. 2). This suggests that hydrochar facilitates faster microbial activity during early digestion stages. The hydrochar can act as an electrical conductor, promoting DIET, thereby enhancing the rate of electron exchange between fermentative bacteria and methanogenic archaea, and accelerate methane [16].

When evaluating the effects of hydrochar type on methane yield over the 35-day digestion period, WO exhibited similar methane content and yield regardless of hydrochar type. This contrasts with lignocellulosic and starchy biomasses, where HD addition resulted in higher methane yields than HL by 20.02 %, 23.22 %, and 13.72 % for GS-150, SR-150, and LCR-150, respectively. However, the difference was not statistically significant for SR-150. Notably, HL-treated samples showed greater variability, with standard deviations 2.5, 1.9, and 1.4 times higher than those of HD for GS-150, SR-150, and LCR-150, respectively. This trend persisted across repeated trials. Methane production among replicates was relatively consistent during the first 10 days for both hydrochar types; however, after day 10, increased variability was observed in HL treatments. These findings suggest that HD provided more stable process performance, which is critical for long-term AD operation.

The superior methane yield observed with HD compared to HL can be attributed to a combination of physicochemical properties that favor microbial activity and direct interspecies electron transfer. HD exhibited significantly higher electrical conductivity (8.21 mS/cm), 60.7 % greater than HL (5.11 mS/cm), primarily due to its elevated ash content (36.8 %) and the presence of elements such as Fe (0.659 %), Ca (12.58

%), Mg (2.76 %), and Mn (0.099 %). Fe can mediate electron flow through reversible Fe(II)/Fe(III) redox cycling [28].  $\text{Ca}^{2+}$  and  $\text{Mg}^{2+}$  promotes microbial adhesion via ionic bridging [29]. Mn biostimulates the growth of methanogenic bacteria and enhances substrate hydrolysis-acidification [30]. Together, these properties enhance ionic mobility and electron transfer, strengthening DIET efficiency and ultimately increasing methane production in HD compared to HL.

Additionally, HD exhibited a rougher surface texture (Fig. 3), as well as higher surface area, total pore volume, and average pore diameter—4.73, 5.79, and 1.30 times greater than HL, respectively—promoting greater microbial attachment [31] and methanogenic community diversity [12], thereby enhancing substrate accessibility and conversion efficiency. Although HL contained higher fixed carbon (41.36 %) and a greater thermostable fraction, making it more suitable for long-term carbon sequestration, its limited porosity and lower EC likely constrained microbial interactions during anaerobic digestion. Furthermore, FTIR analysis (Table 6 and Figure S-2) showed that both HL and HD shared typical functional groups such as O–H ( $\sim 3433 \text{ cm}^{-1}$ ) and C=O/C=C ( $\sim 1628$  and  $1514 \text{ cm}^{-1}$ ), indicating carboxylic groups. Notably, HD exhibited a unique peak at  $1385 \text{ cm}^{-1}$ , suggesting a higher abundance of carboxylic functionalities that enhance microbial attachment and electron transfer. Additionally, HD showed stronger C–O stretching ( $1018 \text{ cm}^{-1}$ ) and aromatic C–H bending ( $876$ ,  $667 \text{ cm}^{-1}$ ), absent in HL, indicating more complex aromatic structures and richer surface chemistry. These characteristics are known to support DIET, likely contributing to HD's superior performance in enhancing methanogenesis. These combined properties of HD—conductivity, porosity, and surface functionality—contributed to a more favorable environment for methanogenesis, ultimately resulting in a higher methane yield compared to HL.

This study demonstrates that HD, derived from the digestate of a

**Table 3**  
Characteristics of pretreated biomass.

Pretreated biomass	Mixed solid and liquid (%)				Liquid fraction (mg/L)		
	pH	TS	VS	Ash	Sugar	Organic acids	Furfural, 5-HMF
GS-50	6.10 ± 0.01	13.56 ±0.70	12.61 ±0.68	0.94 ±0.02	G = 59.16 ± 1.28 X = 147.86 ± 3.45	L = ND F = ND Ac = ND P = ND Ib = ND B = ND Iv = ND V = ND Ic = ND H = 218.66 ± 5.96	ND, ND
GS -100	5.77 ± 0.01	13.69 ±0.49	12.64 ±0.46	1.03 ±0.01	G = 86.04 ± 0.99 X = 160.53 ± 2.39 A = 159.63 ± 2.36	L = ND F = ND Ac = ND P = ND Ib = 58.81 ± 3.44 B = ND Iv = 105.43 ± 36.42 V = ND Ic = ND H = ND	173.58 ± 2.48 185.90 ± 41.6
GS -150	4.74 ± 0.01	12.50 ±0.38	11.34 ±0.31	1.20 ±0.06	G = 79.69 ± 1.83 X = 373.51 ± 1.50 A = 464.25 ± 6.19	L = ND F = 19.45 ± 0.70 Ac = 34.88 ± 1.24 P = ND Ib = 21.71 ± 3.09 B = ND Iv = 88.06 ± 6.41 V = ND Ic = ND H = ND	456.33 ± 13.61 272.09 ± 7.59
SR-50	4.88 ±0.01	16.91 ±2.28	16.66 ±2.81	0.25 ±0.04	G = 500.00–800.00 X = 124.70 ± 3.16	L = ND F = 25.99 ± 1.90 Ac = ND P = ND Ib = ND B = ND Iv = ND V = ND Ic = ND H = ND	ND, ND
SR-100	6.37 ±0.01	10.97 ±2.40	10.93 ±2.39	0.03 ±0.00	N/A	N/A	N/A
SR-150	4.94 ±0.01	13.21 ±0.10	13.17 ±0.12	0.07 ±0.01	G = 262.87 ±1.64	L = 122.85 ± 4.87 F = 209.35 ± 1.31 Ac = ND P = 51.45 ± 1.14 Ib = ND B = 22.32 ± 2.26 Iv = ND V = 175.69 ± 5.13 Ic = ND H = ND	151.27 ± 6.66 271.06 ± 1.50
LCR-50	6.03 ±0.01	11.97 ±0.38	11.84 ±0.43	0.13 ±0.06	G = 286.81 ±6.16	L = ND F = ND Ac = ND P = ND Ib = ND B = ND Iv = ND V = ND Ic = ND H = ND	ND, ND
LCR-100	6.25 ±0.01	12.67 ±0.38	12.40 ±0.39	0.25 ±0.00	N/A	N/A	N/A
LCR-150	4.70 ±0.01	12.65 ±0.07	12.59 ±0.09	0.06 ±0.02	G = 552.72 ±32.33	L = 116.28 ± 8.45 F = 359.87 ± 14.21 Ac = ND P = 58.05 ± 0.07 Ib = ND B = 21.17 ± 0.44 Iv = ND V = 374.03 ± 6.12	154.26 ± 4.78 428.55 ± 9.26

(continued on next page)

**Table 3** (continued)

Pretreated biomass	Mixed solid and liquid (%)				Liquid fraction (mg/L)		
	pH	TS	VS	Ash	Sugar	Organic acids	Furfural, 5-HMF
						Ic = ND H = ND	

Note: Grass silage, GS; Spoiled rice, SR; Left-over cooked rice, LCR; Glucose, G; Xylose, X; Arabinose, A; Levulinic acid, L; Formic acid, F; Acetic acid, Ac; Propionic acid, P; Isobutyric acid, Ib; Butyric acid, B; Isovaleric acid, Iv; Valeric acid, V; Isocaproic Acid, Ic; Hexanoic acid, H; The concentration of glucose (G) in the liquid fraction of SR-50 exhibited a high standard deviation, therefore, the data is presented as a range to better represent its variability.

**Table 4**

Kinetic parameters of anaerobic digestion of untreated and pretreated biomass derived from Modified Gompertz Models.

Pretreatments	Modified Gompertz model		
	$P$ (L CH <sub>4</sub> /kg-VS)	$R_m$ (L CH <sub>4</sub> /kg-VS/day)	$\lambda$ (days)
Un-GS	145.92 ± 2.53	8.69 ± 0.34	1.15 ± 0.04
GS-50	136.34 ± 14.23	8.58 ± 0.73	1.06 ± 0.14
GS-100	154.52 ± 7.12	8.70 ± 0.15	0.78 ± 0.05
GS-150	179.09 ± 3.78	11.68 ± 0.50	0.32 ± 0.11
Un-SR	292.73 ± 1.21	18.93 ± 0.76	2.76 ± 0.20
SR-50	139.74 ± 16.97	17.58 ± 2.98	0.89 ± 0.29
SR-100	184.22 ± 5.68	15.94 ± 1.61	2.54 ± 0.39
SR-150	210.07 ± 22.39	14.79 ± 2.86	4.76 ± 0.08
Un-LCR	272.13 ± 2.63	13.47 ± 0.83	3.65 ± 0.47
LCR-50	240.74 ± 15.06	10.71 ± 2.16	16.89 ± 4.16
LCR-100	228.14 ± 15.79	14.37 ± 1.74	3.16 ± 0.17
LCR-150	261.13 ± 3.98	21.22 ± 3.42	11.08 ± 0.37
WO (35 days)	445.81 ± 24.90	22.53 ± 1.14	7.92 ± 0.38
WO (58 days)	499.96 ± 15.95	21.89 ± 1.65	7.77 ± 0.04

Note: The first-order model yielded  $R^2$  values 0.8218–0.8939, while the modified Gompertz model achieved  $R^2$  values ranging from 0.9813 to 0.9997.

grass-fed biogas power plant, more effectively enhanced anaerobic digestion performance than HL, which was produced from external *Leucaena* residues. These results support the internal reuse of digestate for HD production, promoting a bio-circular economy within the biogas plant while sustaining higher methane yields. However, the observed enhancement in methanogenesis was limited to the early digestion phase and did not increase cumulative methane yield over 35 days, consistent with Başar et al. [15], who reported similar trends with biochar addition. This decline may be attributed to excessive hydrochar loading. Therefore, the subsequent section evaluates the effects of varying HD dosages to determine the optimal rate for maximizing methane production.

### 3.3. Effect of HD hydrochar dosage on anaerobic digestion behavior

The results in Fig. 4 demonstrate that adding 10 % hydrochar combined with 150 °C pretreatment significantly enhanced early-stage methanogenesis across all biomass types, as indicated by shorter  $\lambda$  values compared to lower hydrochar dosages. Increasing hydrochar from 2.5 % to 5 % yielded minimal improvement, whereas increasing from 5 % to 10 % substantially shortened the lag phase for pretreated SR, LCR, and WO—from 19.62, 19.64, and 7.71 days to 1.69, 1.38, and 3.32 days, respectively. Notably, even 2.5 % hydrochar was sufficient to initiate immediate methane production. Similar lag phase reductions have been observed in digestion of activated sludge [39] and tofu residue [40]. Shortening the lag phase offers operational advantages by reducing AD residence time, thus enabling smaller reactor volumes and lowering construction and operating costs in full-scale applications.

Moreover, an interesting observation was noted: SR-HD150-10 and LC-HD150-10, both starchy biomasses, exhibited the highest early cumulative methane yields, reaching 74.63 % and 86.35 % of their final methane production, respectively (Table 7). These substrates

**Table 5**

Kinetic parameters of anaerobic digestion with hydrochar addition derived from Modified Gompertz Models.

Pretreatments	Modified Gompertz model		
	$P$ (L CH <sub>4</sub> /kg-VS)	$R_m$ (L CH <sub>4</sub> /kg-VS/day)	$\lambda$ (days)
Un-GS	145.92 ± 2.53	8.69 ± 0.34	1.15 ± 0.04
Un-GS-HD-2.5	158.92 ± 3.36	5.26 ± 3.67	2.58 ± 0.31
Un-GS-HD-5	171.70 ± 8.09	5.52 ± 4.14	20.62 ± 0.09
Un-GS-HD-10	166.81 ± 8.41	5.69 ± 4.25	2.81 ± 0.11
GS-150	178.16 ± 4.90	11.90 ± 0.23	0.36 ± 0.06
GS-HD150-2.5	126.40 ± 2.72	9.00 ± 0.16	0
GS-HD150-5	112.50 ± 3.26	8.12 ± 0.47	0
GS-HD150-10	144.64 ± 5.46	10.90 ± 0.16	0
GS-HL-150-10	116.61 ± 10.10	8.93 ± 0.98	0
Un-SR	292.73 ± 1.21	18.93 ± 0.76	2.76 ± 0.20
Un-SR-HD-2.5	314.28 ± 11.89	16.54 ± 2.31	2.98 ± 0.87
Un-SR-HD-5	272.48 ± 46.91	12.91 ± 2.25	2.43 ± 0.28
Un-SR-HD-10	280.58 ± 11.51	13.45 ± 2.28	2.14 ± 1.25
SR-150	210.07 ± 22.39	14.79 ± 2.86	4.76 ± 0.08
SR-HD150-2.5	215.35 ± 48.26	31.09 ± 4.82	19.05 ± 0.14
SR-HD150-5	233.92 ± 14.24	26.77 ± 5.41	19.62 ± 0.43
SR-HD-150-10	137.54 ± 18.09	12.18 ± 2.19	1.69 ± 0.46
SR-HL-150-10	108.61 ± 36.29	4.08 ± 1.50	4.49 ± 2.18
Un-LCR	272.13 ± 2.63	13.47 ± 0.83	3.65 ± 0.47
Un-LCR-HD-2.5	184.08 ± 42.23	13.05 ± 2.64	16.85 ± 1.77
Un-LCR-HD-5	253.29 ± 21.29	28.35 ± 13.47	18.80 ± 0.06
Un-LCR-HD-10	237.86 ± 20.77	20.11 ± 2.08	18.67 ± 0.14
LCR-150	261.13 ± 3.98	21.22 ± 3.42	11.08 ± 0.37
LCR-HD150-2.5	187.36 ± 41.15	23.26 ± 4.54	19.08 ± 0.92
LCR-HD150-5	231.16 ± 10.33	44.14 ± 19.55	19.64 ± 0.66
LCR-HD150-10	130.86 ± 13.73	12.47 ± 1.79	1.38 ± 0.40
LCR-HL-150-10	115.08 ± 10.25	10.02 ± 0.38	1.52 ± 0.26
WO	445.81 ± 24.90	22.53 ± 1.14	7.92 ± 0.38
WO-HD-2.5	424.70 ± 6.09	25.00 ± 0.56	8.55 ± 0.33
WO-HD-5	429.31 ± 7.40	25.02 ± 0.21	7.71 ± 0.07
WO-HD-10	243.11 ± 46.36	12.02 ± 2.00	3.32 ± 0.32
WO-HL-10	239.48 ± 8.56	12.96 ± 2.64	3.23 ± 0.17

Note: The modified Gompertz model achieved  $R^2$  values ranging from 0.974 to 0.999.

demonstrated faster methanogenesis compared to GS-HD150-10 and WO-HD-10, which reached only 15.59 % and 36.66 % of their final yields, respectively. The superior early performance of starchy biomasses is attributed to their higher biodegradability; when partially disrupted by thermal pretreatment and combined with hydrochar addition, their soluble carbohydrate fractions became rapidly available for microbial conversion. In contrast, GS, as a lignocellulosic biomass, retained more recalcitrant solids even after pretreatment. While its liquid fraction provided readily available sugars and organic acids that could be quickly metabolized with hydrochar stimulation, the conversion of the remaining solid fraction required further hydrolysis into soluble intermediates such as glucose and xylose before entering methanogenesis. This limited rapid methane production to only 2 days, the shortest among all tested substrates. Overall, these findings confirm

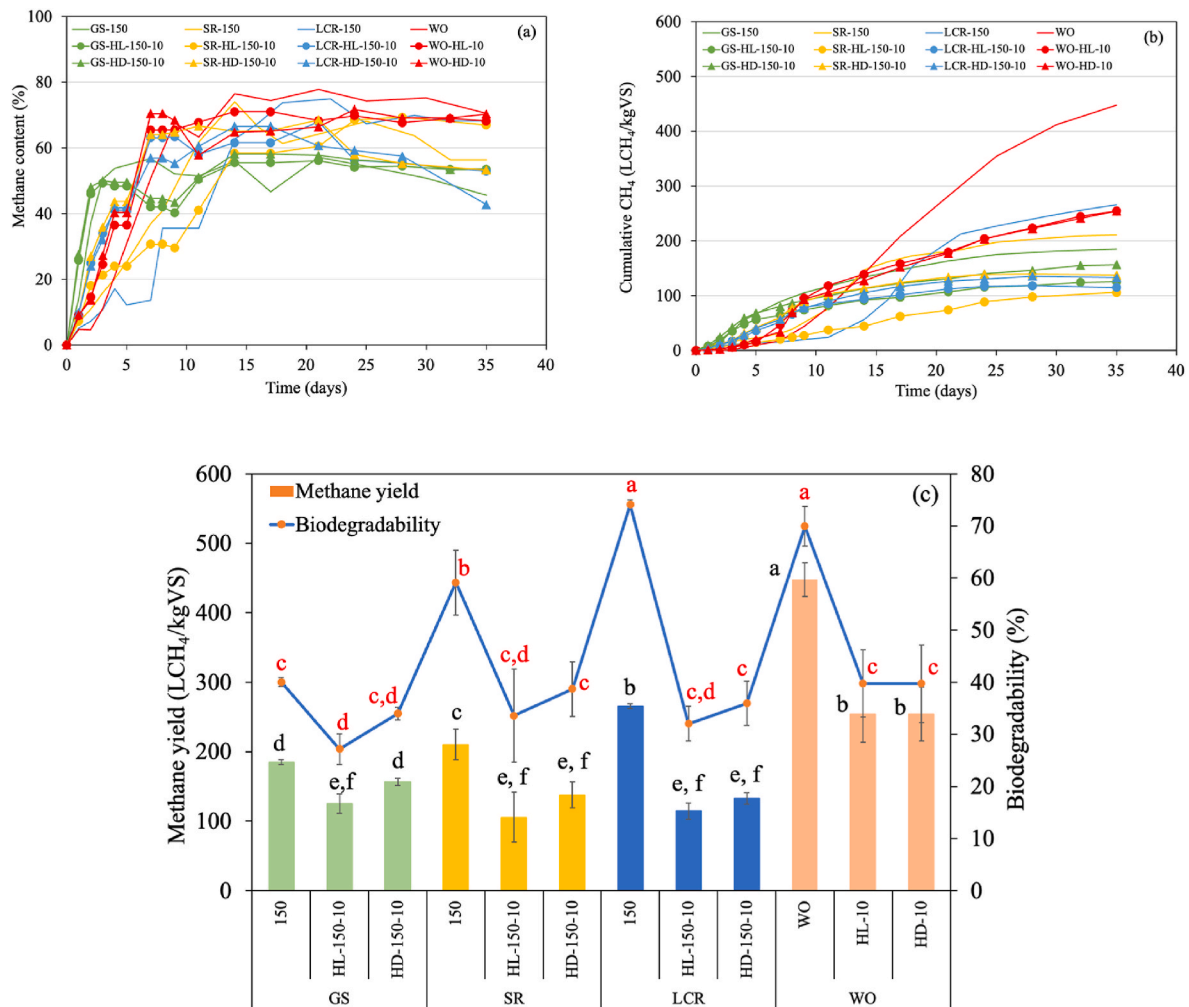


**Fig. 2.** Methane content (a), cumulative methane yield (b), and cumulative methane yield with biodegradability (c) during 35 days of anaerobic digestion of biomass hydrothermally pretreated at 150 °C with 10 % hydrochar addition. Note: Different letters indicate significant differences with  $p \leq 0.05$  for methane yield.

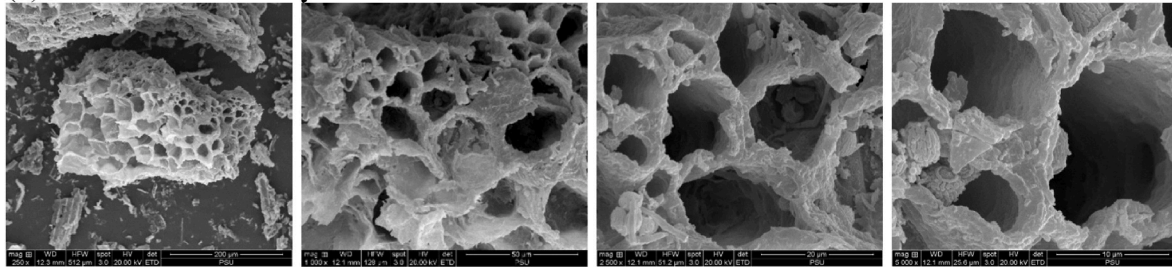
that both hydrothermal pretreatment at 150 °C and 10 % hydrochar addition are key factors for accelerating early-stage methanogenesis, though their effects vary depending on the chemical characteristics of each biomass type.

Although the synergistic application of hydrothermal pretreatment (150 °C) and hydrochar addition (10 %) enhanced early-stage methane production, it led to a reduction in cumulative methane yield over the 35-day anaerobic digestion period. For SR and LCR, methane yields from hydrothermal pretreated samples with hydrochar addition were lower than those from untreated samples, regardless of hydrochar addition. In contrast, GS benefited from either hydrothermal pretreatment at 150 °C or hydrochar addition alone. This decline in long-term performance is likely due to the combined inhibitory effects introduced by both treatments. Hydrothermal pretreatment generates microbial inhibitors such as furfural, 5-HMF, and organic acids, while hydrochar—particularly that produced via hydrothermal carbonization—may release polycyclic aromatic hydrocarbons [41], phenolic compounds, carboxylic acids and furans. This aligns with the FTIR analysis of HD, which showed peaks at 1400–1700  $\text{cm}^{-1}$  and 3500–2500  $\text{cm}^{-1}$ , corresponding to C=C or C=O stretching and O-H stretching in carboxylic groups. Additional peaks were observed at 1000–1200  $\text{cm}^{-1}$  and 1275–1200  $\text{cm}^{-1}$ , representing C–O and C–H functional groups of phenolic compounds. Meanwhile, furans (furfural and 5-HMF) in the liquid from the last day of digestion were 450.32 mg/L (GS-HD150-10), 139.05 mg/L (SR-HD150-10), and  $138.88 \pm 0.29$  mg/L (LCR-HD150-10), below the reported inhibitory threshold of 1000 mg/L [42]. However, combined with other inhibitors,

microbial activity could still be affected. Quantitative studies are therefore required to confirm this effect. Additionally, hydrochar also acts as an electron-conductive material, promoting DIET and enhancing the hydrogenotrophic methanogenesis pathway [12]. Excessive hydrochar dosage (10 % of feedstock) enriched with elements, as discussed in Section 3.2, may overstimulate DIET by supplying excess electrons, thereby favoring hydrogenotrophic methanogens. This shift can suppress the activity of acetoclastic methanogens, which normally convert acetate to methane efficiently, leading to a reduced methane yield during the later stages of digestion. These observations are consistent with previous findings which reported that elevated levels of elements such as Ca, Cu, Zn, K, and Mn can result in a reduction in methane yield [15,43].

Similarly, for WO, methane production decreased 1.73-fold as hydrochar dosage increased from 5 % to 10 %. This aligns with Choe et al. (2019), who observed methane yield from fish waste dropped from 219 to 42 L/kg VS when bamboo-derived hydrochar dosage increased from 1:2 to 1:4 (feedstock:hydrochar ratio). Taken together, these results indicate that while the combined application of hydrothermal pretreatment and hydrochar may suppress long-term methane yields, hydrochar addition alone improved or maintained methane yield across all substrates, and for GS it provided an alternative to hydrothermal pretreatment. Optimized hydrochar dosages—5 % for Un-GS and Un-LCR, 2.5 % for Un-SR, and 5 % for WO—were sufficient to improve methane yields by 19.23 % and 7.37 % for Un-GS and Un-LCR, respectively, while maintaining yields for SR and WO. These adjustments



(a) *Leucaena* derived hydrochar

(b) Digestate derived hydrochar

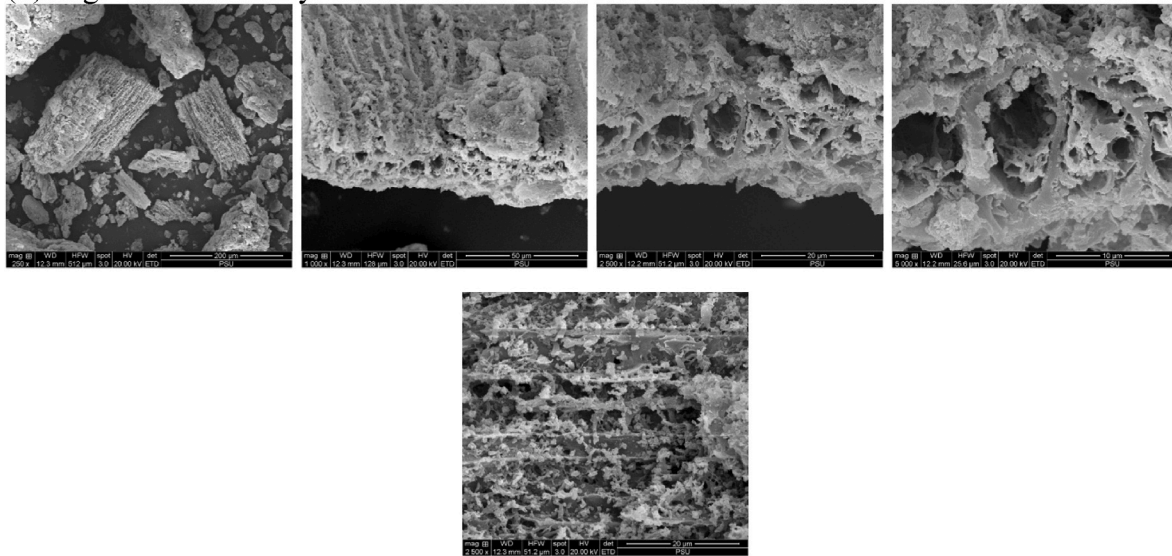
Fig. 3. Scanning electron microscopy of (a) *Leucaena* residue derived hydrochar (b) digestate derived hydrochar.

Table 6

Comparison of functional groups in HL and HD using FTIR Spectroscopy.

Wavenumber (cm <sup>-1</sup> )	Wavenumber HL (cm <sup>-1</sup> )	Wavenumber HD (cm <sup>-1</sup> )	Bond	Functional group	Reference
3500–2500	3433	3433	O-H stretching	carboxylic groups	[32,33]
1400–1700	1628, 1514	1628, 1514, 1385	C=C C=O stretching	carboxylic groups	[32–35]
1275–1200	1273	1273	C–H	phenols	[36]
1000–1200	1116	1116, 1018	C–O stretching	alcohols, phenols	[32,37]
900–665	–	876, 667	Aromatic C–H bending	–	[35,38]

support improved digestate quality for use as a soil amendment and promote long-term carbon sequestration.

Based on these outcomes, biogas power plants may consider two practical operational strategies:

1. Approach I: This approach is suitable for facilities equipped with hydrothermal pretreatment units; thermal conditioning at 150 °C significantly enhances methane yield from GS but is not recommended for starchy biomass (SR and LCR), where pretreatment offers limited benefit.
2. Approach II: This approach applies to facilities capable of producing hydrochar and targeting both methane yield improvement and carbon sequestration. The recommended conditions are:
  - Un-GS with 5 % hydrochar addition (methane yield = 179.34 ± 8.16 LCH<sub>4</sub>/kg VS)
  - Un-SR with 2.5 % hydrochar addition (methane yield = 315.48 ± 12.58 LCH<sub>4</sub>/kg VS)

- Un-LCR with 5 % hydrochar addition (methane yield = 254.07 ± 20.93 LCH<sub>4</sub>/kg VS)
- WO with 5 % hydrochar addition (methane yield = 439.29 ± 5.23 LCH<sub>4</sub>/kg VS)

These findings offer practical insights for optimizing biogas production from diverse organic wastes while supporting circular bioeconomy principles and advancing carbon sequestration objectives in biogas power plants. A further evaluation of Approach II in terms of carbon sequestration potential is presented in Section 3.4.

#### 3.4. Anaerobic digestion and nature-based carbon sequestration approach

In this section, Approach II is further evaluated for its carbon sequestration potential. The potential for carbon sequestration is calculated based on the amount of fixed carbon contained in the hydrochar, which reflects its long-term stability in soil. Applying

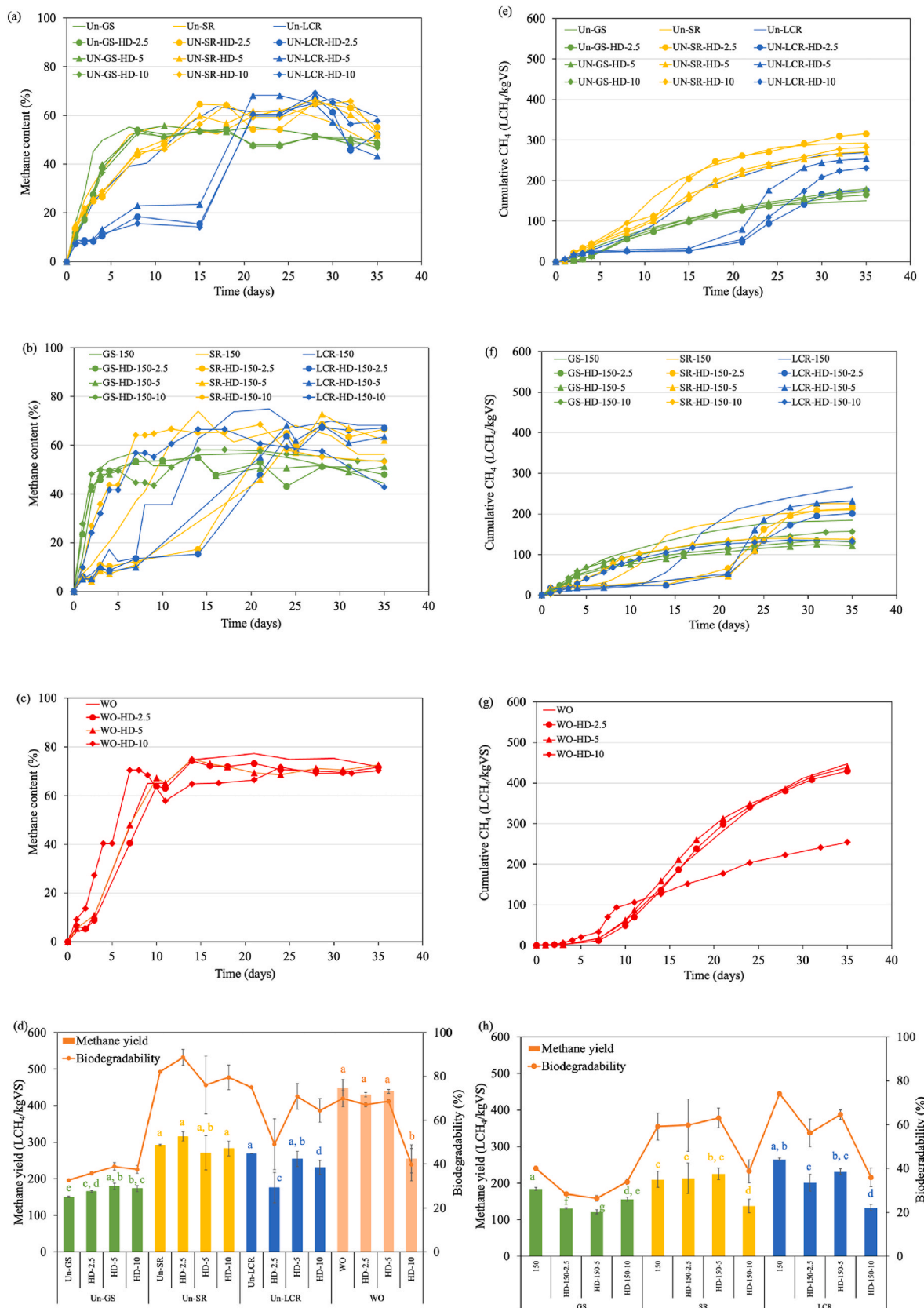


**Fig. 4.** Methane content (a–c), cumulative methane yield (e–g), and cumulative methane yield with biodegradability (d, h) during 35 days of anaerobic digestion of untreated and hydrothermally pretreated (150 °C) biomass with varying dosages of hydrochar additive.

**Table 7**

Methane content and methane yield of 10 % hydrochar addition into anaerobic digestion.

Biomass	Incubation time (day)	CH <sub>4</sub> content (%)	Cumulative CH <sub>4</sub> yield (L CH <sub>4</sub> /kg VS)	% of final CH <sub>4</sub> yield (day 35)
GS-HD150-10	2	48.09 ± 0.52	24.41 ± 0.66	15.59
SR-HD150-10	11	66.66 ± 2.77	102.80 ± 13.90	74.63
LCR-HD150-10	14	68.87 ± 3.05	111.27 ± 10.00	86.35
WO-HD-10	9	68.40 ± 4.55	93.22 ± 20.89	36.66

Note: Data in this table are derived from experimental measurements.; Incubation time refers to the day on which both methane content and cumulative methane yield exceeded those of the control and the treatments with 2.5 % and 5.0 % hydrochar addition.; CH<sub>4</sub> content (%) and cumulative CH<sub>4</sub> yield (L CH<sub>4</sub>/kg VS) are values at the specified incubation time shown in the table.; % of Final CH<sub>4</sub> yield refers the proportion of cumulative methane yield achieved by the specified incubation day, relative to the cumulative methane yield measured on day 35.

hydrochar at the recommended levels in this study could result in the sequestration of at least 5.8 kg carbon/ton dry feedstock (Table 8). Simultaneously, the digestate enriched with hydrochar can serve directly as a soil amendment without concerns about phytotoxicity [13]. This is because the residual compounds generated during hydrothermal carbonization are leached and degraded during anaerobic digestion, rendering the final digestate safe for agricultural use. Thus, digestate with hydrochar contributes both to nature-based carbon sequestration and soil organic carbon fertility improvement.

A life cycle assessment (LCA) is essential to evaluate the overall sustainability of this integrated system, particularly considering the energy demands of both hydrothermal pretreatment and hydrothermal carbonization. While pretreatment operates at moderate temperatures (~150 °C) and HTC at higher temperatures (~265 °C), the use of solar thermal energy as a renewable heat source for both processes could substantially reduce fossil energy consumption and associated environmental impacts [44,45]. Future research should focus on developing integrated decision support tools that combine LCA, life cycle costing—with carbon sequestration benefits of the digestate explicitly included in value assessment—and process performance indicators. Such tools would support multi-objective optimization of methane yield, carbon sequestration potential, economic feasibility, and environmental sustainability in biogas systems.

#### 4. Conclusion

This study demonstrates that integrating hydrochar addition into anaerobic digestion can improve methane production and promote carbon sequestration in biogas power plants. While hydrothermal pretreatment at 150 °C enhanced methane yield for GS, but reduced performance for starchy residues. In contrast, hydrochar addition alone improved or maintained methane yield across all substrates (GS, LCR, SR and WO), and for GS it provided an alternative to hydrothermal pretreatment. Optimal hydrochar dosages—5 % for Un-GS and Un-LCR, 2.5 % for Un-SR, and 5 % for WO—proved effective in boosting or maintaining methane yields. HD outperformed HL due to its superior physicochemical properties. This supports the internal reuse of digestate for HD production, thereby promoting a bio-circular economy within the biogas plant. Overall, this research offers a pathway toward sustainable, carbon-efficient biogas plant systems.

#### CRediT authorship contribution statement

**Apatorn Khongyari:** Writing – original draft, Visualization, Methodology, Investigation, Formal analysis. **Navadol Laosiripojana:** Writing – original draft, Conceptualization. **Santhana Krishnan:** Writing – original draft, Visualization. **Suchewan Yoyurub:** Writing – original draft, Methodology, Conceptualization. **Boonya Charnnok:** Writing – review & editing, Writing – original draft, Visualization, Methodology, Funding acquisition, Formal analysis, Conceptualization.

**Table 8**

Assessment of potential nature-based carbon sequestration with hydrochar addition into anaerobic digestion of various biomass (1 ton dry biomass).

Biomass	Hydrochar addition	Hydrochar addition	Potential carbon sequestered for long term
	%	kg	(kg)
Un-GS	5	50	11.6
Un-SR	2.5	25	5.8
Un-LCR	5	50	11.6
WO	5	50	11.6

Note: Grass silage, GS; Spoiled rice, SR; Left-over cooked rice, LCR; Waste oil, WO; Fixed carbon content 23.1 % dry hydrochar was used to calculate potential carbon sequestered for long term.

#### Availability of data and materials

Data will be made available on request.

#### Funding

This work was supported by National Science, Research and Innovation Fund (NSRF) and Prince of Songkla University (Ref. No. ENG6701039S) and the Graduate School of Prince of Songkla University.

#### Competing interests

The authors declare that they have no known competing financial interests or personal relationships that could have appeared to influence the work reported in this paper.

#### Acknowledgement

This research was supported by National Science, Research and Innovation Fund (NSRF) and Prince of Songkla University (Ref. No. ENG6701039S), and the Graduate School of Prince of Songkla University, Thailand. The authors would also like to recognize the support provided by the Biowaste to Value Laboratory (Energy Park Complex, Energy Systems Research Institute); the Office of Scientific Instrument and Testing; Department of Chemical Engineering; Faculty of Engineering; Faculty of Environmental Management, Prince of Songkla University.

#### Appendix A. Supplementary data

Supplementary data to this article can be found online at <https://doi.org/10.1016/j.biombioe.2025.108431>.

#### Data availability

Data will be made available on request.



## References

- [1] T. Rangseesuriyachai, J. Boonnorat, N. Glanpracha, W. Khetkorn, P. Thiamngoen, K. Pinpathanapong, Anaerobic co-digestion of elephant dung and biological pretreated Napier grass: synergistic effect and kinetics of methane production, *Biomass Bioenergy* 175 (2023), <https://doi.org/10.1016/j.biombioe.2023.106849>.
- [2] U. Jomnonkhaow, S. Sittijunda, A. Reungsang, Influences of size reduction, hydration, and thermal-assisted hydration pretreatment to increase the biogas production from Napier grass and Napier silage, *Bioresour. Technol.* 331 (2021), <https://doi.org/10.1016/j.biortech.2021.125034>.
- [3] B. Charnnok, N. Laosiripojana, Integrative process for rubberwood waste digestibility improvement and levulinic acid production by hydrothermal pretreatment with acid wastewater conversion process, *Bioresour. Technol.* (2022) 127522, <https://doi.org/10.1016/j.biortech.2022.127522>.
- [4] N. Samadamaeng, C. Sawatdeenarunat, B. Charnnok, Enhancing biogas production from cattle manure: a circular economy approach with solar thermal pretreatment and soil conditioning, *J. Environ. Manag.* 368 (2024), <https://doi.org/10.1016/j.jenvman.2024.122086>.
- [5] A. Ismail, F. laqa Kakar, E. Elbeshbishy, G. Nakhla, Combined thermal hydrolysis pretreatment and anaerobic co-digestion of waste activated sludge and food waste, *Renew. Energy* 195 (2022) 528–539, <https://doi.org/10.1016/j.renene.2022.06.042>.
- [6] C. Bougrier, J.P. Delgenès, H. Carrère, Impacts of thermal pre-treatments on the semi-continuous anaerobic digestion of waste activated sludge, *Biochem. Eng. J.* 34 (2007) 20–27, <https://doi.org/10.1016/j.bej.2006.11.013>.
- [7] M.J. Cueto, X. Gómez, M. Otero, A. Morán, Anaerobic digestion and co-digestion of slaughterhouse waste (SHW): influence of heat and pressure pre-treatment in biogas yield, *Waste Manag.* 30 (2010) 1780–1789, <https://doi.org/10.1016/j.wasman.2010.01.034>.
- [8] L.C. Ferreira, T.S.O. Souza, F. Fdz-Polanco, S.I. Pérez-Elvira, Thermal steam explosion pretreatment to enhance anaerobic biodegradability of the solid fraction of pig manure, *Bioresour. Technol.* 152 (2014) 393–398, <https://doi.org/10.1016/j.biortech.2013.11.050>.
- [9] J. Lee, K.Y. Park, Impact of hydrothermal pretreatment on anaerobic digestion efficiency for lignocellulosic biomass: influence of pretreatment temperature on the formation of biomass-degrading byproducts, *Chemosphere* 256 (2020) 127116, <https://doi.org/10.1016/j.chemosphere.2020.127116>.
- [10] C. Veluchamy, A.S. Kalamdhad, Enhancement of hydrolysis of lignocellulose waste pulp and paper mill sludge through different heating processes on thermal pretreatment, *J. Clean. Prod.* 168 (2017) 219–226, <https://doi.org/10.1016/j.jclepro.2017.09.040>.
- [11] N. Chen, X. Zhang, L. Qi, F. Gao, G. Wu, H. Li, W. Guo, H.H. Ngo, Enhancement of volatile fatty acids degradation and rapid methanogenesis in a biochar-assisted anaerobic membrane bioreactor via enhancing direct interspecies electron transfer, *J. Environ. Manag.* 380 (2025), <https://doi.org/10.1016/j.jenvman.2025.125045>.
- [12] J. Bu, Y. Wang, Y. Gao, Q. Zhao, Y. Luo, Y.W. Tjong, H.T. Lam, J. Zhang, Y. He, C.-H. Wang, Y.W. Tong, Enhancing anaerobic digestion of food waste with chemically vapor-deposited biochar: effective enrichment of Methanosarcina and hydrogenotrophic methanogens, *Bioresour. Technol.* 424 (2025) 132225, <https://doi.org/10.1016/j.biortech.2025.132225>.
- [13] D. Bona, D. Bertoldi, G. Borgonovo, S. Mazzini, S. Ravasi, S. Silvestri, C. Zaccane, B. Giannetta, F. Tambone, Evaluating the potential of hydrochar as a soil amendment, *Waste Manag.* 159 (2023) 75–83, <https://doi.org/10.1016/j.wasman.2023.01.024>.
- [14] U. Choe, A.M. Mustafa, H. Lin, J. Xu, K. Sheng, Effect of bamboo hydrochar on anaerobic digestion of fish processing waste for biogas production, *Bioresour. Technol.* 283 (2019) 340–349, <https://doi.org/10.1016/j.biortech.2019.03.084>.
- [15] İ.A. Başar, C. Eskicioglu, N.A. Perendeci, Biochar and wood ash amended anaerobic digestion of hydrothermally pretreated lignocellulosic biomass for biorefinery applications, *Waste Manag.* 154 (2022) 350–360, <https://doi.org/10.1016/j.wasman.2022.10.014>.
- [16] Q. Xu, G. Yang, X. Liu, J.W.C. Wong, J. Zhao, Hydrochar mediated anaerobic digestion of bio-wastes: advances, mechanisms and perspectives, *Sci. Total Environ.* 884 (2023), <https://doi.org/10.1016/j.scitotenv.2023.163829>.
- [17] B. Charnnok, K. Khompatara, S. Chairapat, S. Krishnan, Hydrothermal carbonization of digestate from lignocellulosic biogas power plants for sustainable soil improvement and low carbon emissions, *Bioenergy Res.* 18 (2025), <https://doi.org/10.1007/s12155-025-10865-5>.
- [18] P. Pengpit, S. Chotchutima, S. Chairapat, S. Soyurub, B. Charnnok, Enhancing bioenergy and feed production in Southern Thailand: an approach through *Leucaena* cultivation and hydrothermal carbonization, *Renew. Energy* 237 (2024), <https://doi.org/10.1016/j.renene.2024.121673>.
- [19] F. Raposo, C.J. Banks, I. Sievert, S. Heaven, R. Borja, Influence of inoculum to substrate ratio on the biochemical methane potential of maize in batch tests, *Process Biochem.* 41 (2006), <https://doi.org/10.1016/j.procbio.2006.01.012>.
- [20] A.M. Buswell, H.F. Mueller, Mechanism of methane fermentation, *Ind. Eng. Chem.* 44 (1952), <https://doi.org/10.1021/ie50507a033>.
- [21] D. Deublein, A. Steinhauser, *Biogas from Waste and Renewable Resources*, second, WILEY-VCH, 2011.
- [22] E. Antwi, N. Engler, M. Nelles, A. Schüch, Anaerobic digestion and the effect of hydrothermal pretreatment on the biogas yield of cocoa pods residues, *Waste Manag.* 88 (2019), <https://doi.org/10.1016/j.wasman.2019.03.034>.
- [23] K. Nunui, P. Boonsawang, S. Chairapat, B. Charnnok, Using organosolv pretreatment with acid wastewater for enhanced fermentable sugar and ethanol production from rubberwood waste, *Renew. Energy* 198 (2022) 723–732, <https://doi.org/10.1016/j.renene.2022.08.068>.
- [24] Y. Li, S.K. Khanal, *Bioenergy : Principles and Applications*, Wiley Blackwell, 2017.
- [25] T. Eom, S. Chairapat, B. Charnnok, Enhanced enzymatic hydrolysis and methane production from rubber wood waste using steam explosion, *J. Environ. Manag.* 235 (2019) 231–239, <https://doi.org/10.1016/j.jenvman.2019.01.041>.
- [26] B. Charnnok, R. Sawangkeaw, S. Chairapat, Integrated process for the production of fermentable sugar and methane from rubber wood, *Bioresour. Technol.* 302 (2020) 122785, <https://doi.org/10.1016/j.biortech.2020.122785>.
- [27] Z. Li, S. Qiu, J. Xu, S. Ge, Effect of undissociated n-caproic acid on methanogen activity and subsequent recovery: methane anabolism and community structure, *ACS ES T Eng.* 4 (2024) 706–716, <https://doi.org/10.1021/acsestengg.3c00393>.
- [28] H. Xu, M. Wang, S. Hei, X. Qi, X. Zhang, P. Liang, W. Fu, B. Pan, X. Huang, Neglected role of iron redox cycle in direct interspecies electron transfer in anaerobic methanogenesis: inspired from biogeochemical processes, *Water Res.* 262 (2024), <https://doi.org/10.1016/j.watres.2024.122125>.
- [29] A.J. De Kerckhove, M. Elimelech, Calcium and magnesium cations enhance the adhesion of motile and nonmotile *Pseudomonas aeruginosa* on alginate films, *Langmuir* 24 (2008) 3392–3399, <https://doi.org/10.1021/la7036229>.
- [30] Y.Y. Choong, I. Norli, A.Z. Abdullah, M.F. Yhaya, Impacts of trace element supplementation on the performance of anaerobic digestion process: a critical review, *Bioresour. Technol.* 209 (2016) 369–379, <https://doi.org/10.1016/j.biortech.2016.03.028>.
- [31] Y.L. Jia, W. Hu, C.C. Tang, A.J. Zhou, W. Liu, Z. Chen, Y.X. Ren, Z.W. He, Biochar derived from straw regulate anaerobic digestion: insights into the roles of vegetative organs, *Renew. Energy* 253 (2025), <https://doi.org/10.1016/j.renene.2025.123554>.
- [32] H.G. Zhen, C. Hu, L. Yang, G. Du Laing, Hydrochar produced from mixed feedstocks as efficient adsorbent for selenium and chromium removal from acidic wastewater, *Desalination* 593 (2025), <https://doi.org/10.1016/j.desal.2024.118152>.
- [33] Y. Yu, Z. Lei, X. Yang, X. Yang, W. Huang, K. Shimizu, Z. Zhang, Hydrothermal carbonization of anaerobic granular sludge: effect of process temperature on nutrients availability and energy gain from produced hydrochar, *Appl. Energy* 229 (2018) 88–95, <https://doi.org/10.1016/j.apenergy.2018.07.088>.
- [34] F.A. Dawodu, O. Ayodele, J. Xin, S. Zhang, D. Yan, Effective conversion of non-edible oil with high free fatty acid into biodiesel by sulphonated carbon catalyst, *Appl. Energy* 114 (2014) 819–826, <https://doi.org/10.1016/j.apenergy.2013.10.004>.
- [35] P. Wang, H. Peng, S. Adhikari, B. Higgins, P. Roy, W. Dai, X. Shi, Enhancement of biogas production from wastewater sludge via anaerobic digestion assisted with biochar amendment, *Bioresour. Technol.* 309 (2020), <https://doi.org/10.1016/j.biortech.2020.123368>.
- [36] U. Bordoloi, D. Das, D. Kashyap, D. Patwa, P. Bora, H.H. Muigai, P. Kalita, Synthesis and comparative analysis of biochar based form-stable phase change materials for thermal management of buildings, *J. Energy Storage* 55 (2022), <https://doi.org/10.1016/j.est.2022.105801>.
- [37] G.A. Tafete, A. Uysal, N.G. Habtu, M.K. Abera, T.A. Yemata, K.S. Duba, S. Kinayyigit, Hydrothermally synthesized nitrogen-doped hydrochar from sawdust biomass for supercapacitor electrodes, *Int. J. Electrochem. Sci.* 19 (2024), <https://doi.org/10.1016/j.ijeos.2024.100827>.
- [38] S. Xu, C. Wang, Y. Duan, J.W.C. Wong, Impact of pyrochar and hydrochar derived from digestate on the co-digestion of sewage sludge and swine manure, *Bioresour. Technol.* 314 (2020), <https://doi.org/10.1016/j.biortech.2020.123730>.
- [39] Z. Shi, S. Campanaro, M. Usman, L. Treu, A. Basile, I. Angelidaki, S. Zhang, G. Luo, Genome-centric metatranscriptomics analysis reveals the role of hydrochar in anaerobic digestion of waste activated sludge, *Environ. Sci. Technol.* 55 (2021) 8351–8361, <https://doi.org/10.1021/acs.est.1c01995>.
- [40] U. Choe, A.M. Mustafa, X. Zhang, K. Sheng, X. Zhou, K. Wang, Effects of hydrothermal pretreatment and bamboo hydrochar addition on anaerobic digestion of tofu residue for biogas production, *Bioresour. Technol.* 336 (2021), <https://doi.org/10.1016/j.biortech.2021.125279>.
- [41] T. Liu, L. Tian, Z. Liu, J. He, H. Fu, Q. Huang, H. Xue, Z. Huang, Distribution and toxicity of polycyclic aromatic hydrocarbons during CaO-assisted hydrothermal carbonization of sewage sludge, *Waste Manag.* 120 (2021) 616–625, <https://doi.org/10.1016/j.wasman.2020.10.025>.
- [42] J.R. Kim, K.G. Karthikeyan, Effects of severe pretreatment conditions and lignocellulose-derived furan byproducts on anaerobic digestion of dairy manure, *Bioresour. Technol.* 340 (2021), <https://doi.org/10.1016/j.biortech.2021.125632>.
- [43] M. Zhang, Y. Wang, Effects of Fe-Mn-modified biochar addition on anaerobic digestion of sewage sludge: biomethane production, heavy metal speciation and performance stability, *Bioresour. Technol.* 313 (2020), <https://doi.org/10.1016/j.biortech.2020.123695>.
- [44] J.V. Briongos, S. Taramona, J. Gómez-Hernández, V. Mulone, D. Santana, Solar and biomass hybridization through hydrothermal carbonization, *Renew. Energy* 177 (2021) 268–279, <https://doi.org/10.1016/j.renene.2021.05.146>.
- [45] G. Ischia, D. Castello, M. Orlandi, A. Miotello, L.A. Rosendahl, L. Fiori, Waste to biofuels through zero-energy hydrothermal solar plants: process design, *Chem. Eng. Trans.* 80 (2020) 7–12, <https://doi.org/10.3303/CET2080002>.